Field-induced structures in miscible ferrofluid suspensions with and without latex spheres

M. F. Islam, K. H. Lin, D. Lacoste, T. C. Lubensky, and A. G. Yodh
Department of Physics and Astronomy, University of Pennsylvania, 209 South 33rd Street, Philadelphia, Pennsylvania 19104
(Received 24 September 2002; published 14 February 2003)

We explore magnetic-field-induced ordering and microphase separation of aqueous ferrofluid and of aqueous mixtures of ferrofluid with nonmagnetic latex spheres. The ferrofluid is a surfactant stabilized aqueous suspension of magnetite (Fe_3O_4) particles with average diameter 20 nm (including the ~2.5-nm thick surfactant layer); the nonmagnetic latex spheres are charge stabilized polymethylmethacrylate (PMMA) particles with diameters of 42 nm, 108 nm, and 220 nm. In the presence of a uniform magnetic field, needlelike ferrofluid droplets formed that eventually grew to sample-traversing columns at fields of ~600 G; the two-dimensional structure of these columns was, however, glassy rather than hexagonal. In higher fields, ~1000 G, the columns stretched and coalesced into sheetlike striped liquids, but a true lamellar phase was not observed. The addition of nonmagnetic latex spheres to the ferrofluid suspension lowered substantially the critical field for the formation of columns, and induced lamellar (stripe) phases at relatively low applied fields. Image analysis was used to determine the spatial correlation functions, the average needle or column spacing, and the average lamellae spacing of these samples as a function of latex sphere size and concentration.

DOI: 10.1103/PhysRevE.67.021402 PACS number(s): 82.70.Dd, 75.50.Mm, 61.12.Ex, 75.70.Kw

I. INTRODUCTION

Ferrofluids (FF) are suspensions of small, single domain magnetizable particles with diameters of order of 10 nm. If the ferrofluid is immersed in a magnetic field, a magnetization is induced in the sample, and dipolar interactions between oriented ferrofluid particles become important. When dipolar interactions are sufficiently strong, ferrofluids exhibit a rich phase behavior [1] as a function of external field and volume fraction. The high-field solidlike phases have rheological properties that differ significantly from those of the low-field homogeneous phase, and large changes in system response and rigidity can be produced with relatively modest changes in magnetic field. This switching property has led to useful applications of ferrofluids, from sealants in the rotary shafts of computer disk drives to heat dissipaters in speaker coils [1]. These demonstrated applications and fundamental questions about dipolar liquids and solids have driven extensive theoretical and experimental investigations of the phase behavior of ferrofluids [1–22].

In this paper we focus on the behavior of aqueous miscible ferrofluids and miscible mixtures of ferrofluid and nonmagnetic spheres; our suspending fluid is water, and both the magnetic and nonmagnetic particles are stabilized in water. More commonly, the ferrofluid is composed of magnetic particles suspended in one solvent (e.g., oil) that is then mixed with a second immiscible fluid (e.g., water). An interfacial tension between the two components of the mixture arises naturally in the immiscible samples. This interfacial tension plays a critical role in the energy balance of the system and, ergo in the formation of columnar, lamellar, and labyrinthine phases in magnetic fields [2–15,23].

Even less attention has been afforded to miscible mixtures; the combination of ferrofluid and added nonmagnetic particles represents an important variant upon simple dipolar fluids. To our knowledge, there are no theoretical treatments of this system. There are, however, a few interesting experiments on mixtures. In one limit, which we do not explore in the present study, nonmagnetic particles with relatively large diameter were mixed in ferrofluids having very large magnetic particle volume fractions (i.e., volume fractions of $\geqslant 0.2$) [1,24–26]. The nonmagnetic latex spheres in these systems behaved as magnetic holes [1,24–26], whose interactions induced the formation of chains and two-dimensional (2D) crystals dependent on field direction and sample geometry. In another limit, small nonmagnetic particles were mixed in low volume-fraction ferrofluids [27,28]. The phase behavior of these systems was not reported, but neutron scattering experiments suggested that some anisotropy in the spatial distribution of the nonmagnetic particles was produced through its interaction with the ferrofluid particles. It was further suggested that the ferrofluids might be used to align anisotropic macromolecules.

In this paper, we report experiments on thin (but still three-dimensional) samples of aqueous ferrofluid and of aqueous mixtures of ferrofluid and nonmagnetic particles in magnetic fields. We have studied the phase behavior of these systems directly with optical microscopy. We used image analysis and cycling to determine when the samples reached equilibrium (or at least steady state), and we used image analysis to study long-range order and periodicity in these systems. In very low fields, the pure ferrofluid was isotropic. With increasing field, elongated droplets consisting of regions of increased ferrofluid particle density formed. We refer to these droplets as needles hereafter. Their long axes were parallel to the field. With a further increase in field, the needles grew and eventually stretched from the top to the bottom of the sample. We will call these sample spanning needle columns, and we refer to the transition from predominantly needles to predominantly columns as the isotropic-to-columnar transition. The two-dimensional structure of the columns was glassy rather than hexagonal. At higher fields a disordered striped-liquid phase [29] rather than a true stripe phase formed. The addition of nonmagnetic spheres, with diameters two to ten times the size of the magnetic particles, induced significant new behaviors and structures. The field

strength required for the isotropic-to-columnar transition was reduced substantially relative to that of the pure ferrofluid. In addition, true lamellar (striped) phases formed at a lower field than that required to produce the striped-liquid phase in the pure ferrofluid. This consequence of added particles (i.e., lowering of the transition fields) is qualitatively new and potentially useful. We studied the spatial correlation functions of the columnar and lamellar phases as a function of particle diameter and volume fraction.

II. EXPERIMENT

Our ferrofluid solution was a commercially available product under the trade name EMG 705 from Ferrofluidics Corporations, Nashua, NH. The ferrofluid solution consisted of Fe_3O_4 particles dispersed in water. The ferrofluid particles were stabilized against aggregation by surfactants. We processed the commercial ferrofluid solution to remove excess surfactants without destabilizing the ferrofluid particles and to reduce size polydispersity of the ferrofluid particles. We removed excess surfactants from ferrofluid solution so that excess surfactants could not stabilize any of the structures formed by ferrofluid under magnetic field. For the removal of excess surfactants from the commercial ferrofluid sample, we employed repeated dialysis and redispersion using a stock solution of surfactants obtained from Ferrofluidics. A combination of centrifugation and magnetic size sorting was used to reduce the size polydispersity of the ferrofluid particles [30]. The average ferrofluid particle diameter d_{FF} in the processed sample was 20 nm, and the sample polydispersity was 15%; both numbers were deduced from dynamic light scattering measurements. The nonmagnetic latex spheres were polymethylmethacrylate (PMMA) beads. The average diameter (d_{NM}) and polydispersity of the PMMA beads were measured by dynamic light scattering to be 42 nm and 7%, 108 nm and 6%, and 220 nm and 4%, respectively. The 42 nm PMMA beads were stabilized by 5–8m*M* dodecyl trimethyl ammonium bromide surfactants; the 108 nm and 220 nm PMMA beads were stabilized by embedded amine groups.

In order to determine the magnetic moments of the particles, a dc magnetometer (Physical Property Measurement Systems, Quantum Design, San Diego, CA) was employed to measure the magnetization curves for the ferrofluid, the nonmagnetic spheres, and the mixtures of ferrofluid and nonmagnetic spheres. The samples were housed in 1.3-mm-diameter×1-mm-long cylindrical plastic tubes sealed by parafilm over the open ends. Magnetization measurements were performed from -5 T to 5 T for the nonmagnetic latex spheres, and from -9 T to 9 T for the pure ferrofluid and the mixtures. The samples were kept at room temperature. The diamagnetic susceptibility (χ_{dia}) of the nonmagnetic spheres was calculated to be $-7.19\times10^{-5}\pm0.2\times10^{-6}$, using the slope of a fitted straight line through the measured magnetization curve. A magnetization curve for nonmagnetic spheres is shown in Fig. 1.

In our measurements of ferrofluid alone and the mixtures, we calculated χ_{dia} from the slope of a fitted straight line at high fields (i.e., above ±4.5 T). We then recalculated the magnetization using the expression $M(H)=M(H)_{\mathrm{measured}}-\chi_{\mathrm{dia}}H$. These recalculated curves are plotted in Fig. 1. The effective saturation magnetization M_s was determined from the plateau values of the resultant magnetization curve. The effective saturation magnetization for ferrofluid alone and the mixtures are shown in Fig. 2. The effective saturation magnetization of the ferrofluid particles is $4.84\times10^5\pm4.7\times10^3$ A m^{-1}. Assuming a magnetic core diameter of 15 nm, our ferrofluid particles have a magnetic moment of 8.48×10^{-19} A m^2. Our measurements show that the effective saturation magnetization of ferrofluid particles increases by ~7% as the volume fraction of the added 42-nm nonmagnetic beads increases from 0% to 20%. A substantially weaker increase was also observed as a function of the diameter of the nonmagnetic spheres. These effects were relatively small, but repeatable. We do not as yet have an explanation for why the nonmagnetic spheres appear to increase the saturation magnetization of the ferrofluid particles in

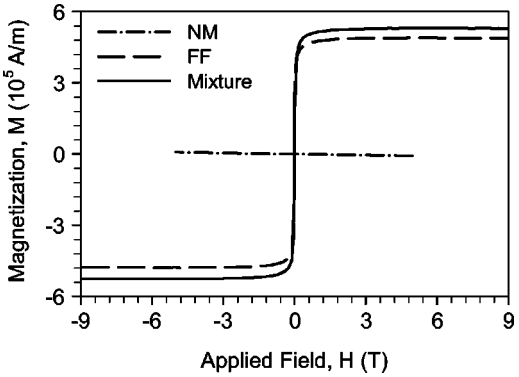

FIG. 1. Magnetization measurement for ferrofluid (FF) alone, for nonmagnetic (100 nm) spheres (NM), and a mixture of ferrofluid ($\phi_{\mathrm{FF}}=0.5\%$) and nonmagnetic spheres ($d_{\mathrm{NM}}=220$ nm, $\phi_{\mathrm{NM}}=20\%$). In the ferrofluid and the mixture cases, we subtracted the diamagnetic contribution from the measured magnetization.

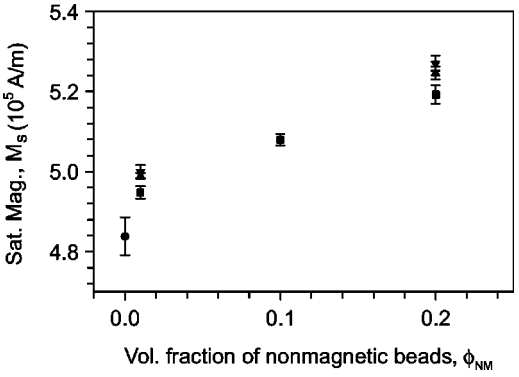

FIG. 2. The saturation magnetization of the ferrofluid for the ferrofluid alone, and for the mixtures of ferrofluid and nonmagnetic spheres. (●) denotes ferrofluid alone, (■) denotes 42-nm NM beads, (▲) denotes 100-nm NM beads, and (▼) denotes 200-nm NM beads. The saturation magnetization increased slightly with increasing volume fraction of the nonmagnetic spheres. The ferrofluid particle volume fraction was fixed at 0.5% for all samples.

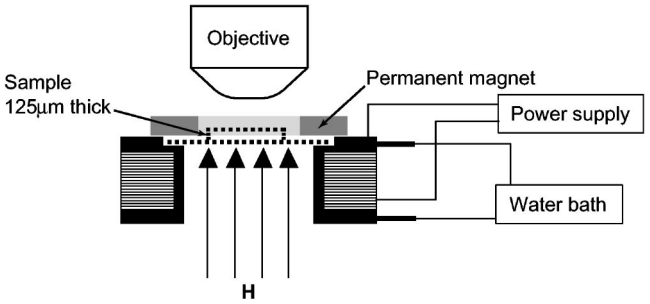

FIG. 3. A schematic of our experimental setup. A water-cooled solenoid and a permanent magnet were used to create the magnetic field. The sample was placed on the top of the solenoid.

these measurements, although we suspect the reason may be connected with the geometry of our sample holder.

The microscope observations were made with suspensions loaded into a sample cell formed by parallel glass plates separated by parafilm spacers of thickness 125 μm. A schematic of our experimental setup and the placement of the sample is shown in Fig. 3. The magnetic field was generated using a water-cooled solenoid and a permanent magnet. The maximum field strength of the solenoid (permanent magnet) was 500 G (670 G). By keeping the sample surface area small, i.e., $\sim$3 mm$\times$3 mm, the applied magnetic field was measured to vary less than 2% across the sample. We placed the sample just above the entrance to the solenoid, and visualized the structures within the sample using a Leica DMIRB inverted optical microscope with a 10$\times$, NA=0.25 air objective.

The samples were imaged using a CCD camera (640$\times$480 pixels; Hitachi, model KP-M1U) and recorded on a S-VHS computer controlled video deck. The video tapes were then digitized and analyzed. To study the ordering of the columns, and to calculate average column or the lamellar spacings, we recorded 2D (top-view) images at a depth of $\sim$60 μm below the sample surface. To obtain better statistics, we used the low magnification objective (10$\times$) so that a large number of columns or lamellar layers were within our field of view (i.e., between 2000–6000 columns or $\gtrsim$50 lamellar layers). We determined the position of the columns (or the lamellar layers) in each image using a centroid technique [31], and then calculated angular averaged pair correlation functions (see Fig. 4). The average column or lamellar spacings were calculated from the position of the first peak of the pair correlation functions. We took four images at different locations at the same depth within the sample to improve the averaging, and then calculated the average column or lamellar spacing.

In order to assess the completeness of needle and columnar structures, we recorded a series of 2D images of the columns (every 1 μm) throughout the sample depth, and then constructed a 3D cube image by stacking these 2D images. Cross sections (side views) through the 3D images parallel to the direction of the applied magnetic field helped us distinguish ferrofluid needles from columns. Note, the needle diameters ranged from 50 to more than 100 particles across.

In the pure ferrofluid experiments, the volume fraction of ferrofluid ϕ_{FF} was maintained at 5×10^{-3}. In the mixture experiments, ϕ_{FF} was fixed at 5×10^{-3}; the volume fraction

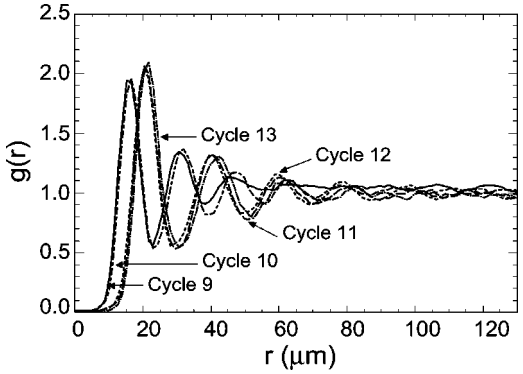

FIG. 4. The pair correlation function of the columnar phase obtained from digitized real space images of 0.5% by volume pure ferrofluid sample at 600 G. After the 11th cycle, the separation between the columns did not change significantly with further cycling of the field. We thus accepted the induced structure as an equilibrium (or steady-state) structure.

of the nonmagnetic particles ϕ_{NM} was varied from 10^{-2} to 1.8×10^{-1}, and d_{NM} was varied from 42 nm to 220 nm.

We used a combination of two methods to ensure the magnetic-field-induced structures reflected equilibrium (or steady-state) behaviors. First, the magnetic field was changed very slowly in all experiments, at a rate of 0.083 G/s. Second, when we reached a field wherein it was desirable to measure an ''equilibrium phase,'' we annealed the system by slowly cycling the field down by $\sim$100 G and then back up again. We cycled the sample many times. The magnetic-field induced structure was determined to be an equilibrium or steady-state structure when the pair correlation function of the image ceased to vary significantly with cycle number. As an example, Fig. 4 shows the two-dimensional pair correlation function for pure ferrofluid as a function of cycle number in its columnar phase at 600 G. The field was cycled 13 times in order to induce an equilibrium or steady-state structure. After inducing an ''equilibrium phase,'' we typically lowered the field to zero again in order to confirm the reversibility of the observed structures.

III. RESULTS AND DISCUSSION

A. Miscible ferrofluid

In this section we discuss observations of the aqueous ferrofluid without added nonmagnetic spheres. Figure 5 is a schematic summarizing the observations. Two sets of images are shown as a function of applied magnetic field. The leftmost set are two-dimensional cross sections of the sample (top view, the magnetic field is perpendicular to the image plane); these images, taken at a depth of $\approx$60 μm into the sample, enable us to visualize ordering of the needles, columns, and sheets in two dimensions. The image set on the right provide side views of the samples, enabling us to determine the needle length. As a group, the data enable us to map out a phase behavior for the pure ferrofluid system as a function of field.

In zero field, no phase separation was observed. We began to observe aggregates at fields of $\sim$90 G. At 100 G these

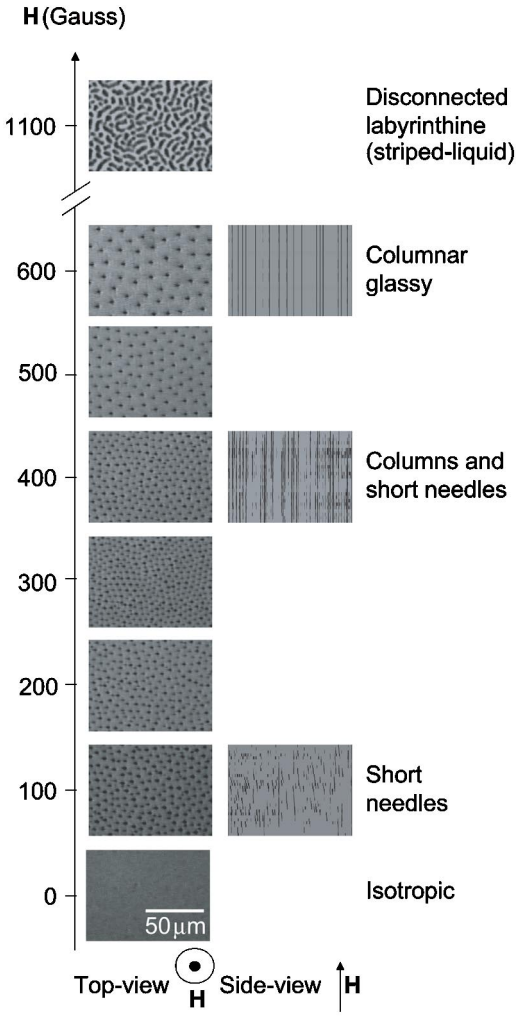

FIG. 5. Optical microscope images of the structures formed by ferrofluid alone in water. A sectioning of a 3D image parallel to the applied magnetic field show an isotropic to needles to columnar progression with increasing field strength. We do not observe stripe and lamellar phases even at $H=1100$ G, but observe a disconnected labyrinthine (striped-liquid [29]) phase at this field.

aggregates are needles, parallel to the applied field and disordered in two-dimensions when viewed from the top down; from the side view it is clear that these needles do not as yet extend fully across the sample. Some of the needles are converted to columns, extending from the top of the sample to the bottom, at 400 G. Almost all needles have been converted to these sample traversing columns by 600 G.

We carried out a battery of image diagnostics in order to ascertain whether the columnar structures were hexagonal or glassy. From the column positions we computed both the pair correlation function $[g(\mathrm{r})]$ and the structure factor $[S(\mathrm{q})]$ for the two-dimensional structure. An example of $g(\mathrm{r})$ for the columnar phase (600 G) is shown in Fig. 4 (cycle 13). The average needle and/or column separation (D) is plotted as a function of magnetic field in Fig. 6. Above 300 G, D increased with increasing magnetic field, indicating an expected increase in the needle or column repulsion with increasing field strength. We next constructed a 2D-Voronoi

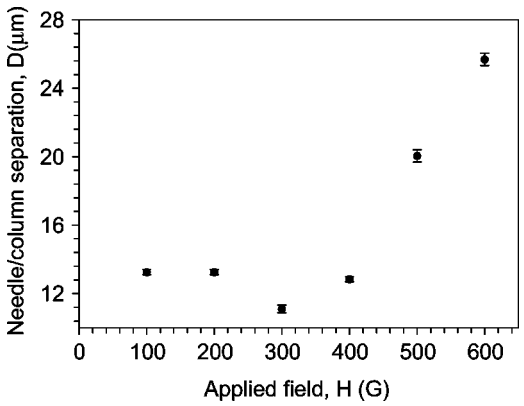

FIG. 6. The average separation between the needles or the columns (D) as a function field strength (H) for ferrofluid alone.

[32] diagram from the center of mass of the columns (at 600 G). The average number of edges in the polygon surrounding each column was between 5 and 6, and approached 6 with increasing magnetic field. The bond-angle order parameter is useful for assessing the degree of long-range order in the sample. It is defined as $\Psi_6=\left|1/N_2\Sigma_{k=1}^{N_2}\Sigma_{j=1}^{N_1}[\mathrm{e}^{6i\theta_j}]\right|$, where θ_j is the angle that the vector between two neighboring columns makes with a fixed axis in the plane, the first summation is over the vertices (N_1) in each Voronoi cell, the second summation is over all of the Voronoi cells (N_2) in the image [33]. Although the bond-angle order parameter increases with increasing magnetic field, it never exceeded 0.1 at any field. This very low value suggests that ferrofluid columns do not possess long-range orientational order. Since the mean-square displacement of the columns was very small, the columnar state is most likely a glassy state of pinned columns, rather than the hexagonal phase predicted by theory.

At the highest-field probed, ~1100 G, the columns merged to form abbreviated sheetlike substructures, which collectively resemble a disconnected labyrinthinelike struc-

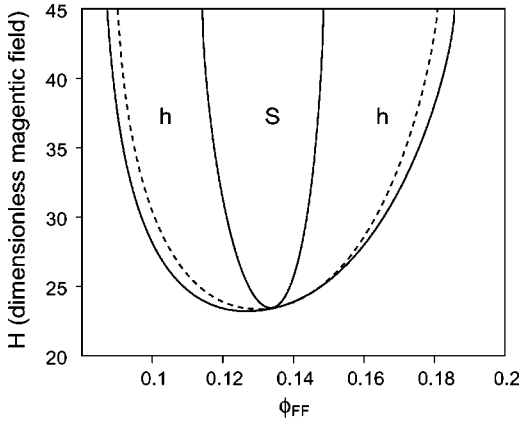

FIG. 7. Assuming a stronger dipolar interaction between the ferrofluid particles ($\lambda=3$), the theoretical phase diagram presented in Ref. [17] (based on the Carnahan-Starling fluid model) predicts no phase transitions at $\phi_{\mathrm{FF}}=0.005$. The theory does not predict any instability of uniform phase for ferrofluid with weaker dipolar interaction either ($\lambda<2.68$), which is our case (λ is 2.2 for our ferrofluid).

ture and the striped liquid of Ref. [29]. The formation of sheetlike structures is somewhat similar to theoretical expectations, although striped and lamellar phases were not observed.

Our observations exhibit qualitative agreement with theories [5,6,16,17] of two-dimensional phase behavior of thin cells that predict transitions from isotropic to hexagonal columnar to stripe phases with increasing field strength at fixed ferrofluid concentration. There are, however, significant qualitative and quantitative discrepancies between our experiments and these theories arising, we believe at least in part from the three-dimensional nature of the experimental system. As in much previous studies on two-dimensional dipolar systems, including ferromagnetic garnets [34,35], type-I superconductors [36], Langmuir films [29,37–39], and ferrofluids [40,41], the two-dimensional patterns we observe are disordered. The columnar (''bubble'') phases were glassy rather than hexagonal, and the striped-liquid phase at high fields was labyrinthine rather than ordered. The origin of this disorder is not entirely clear, though there are indications that it may have to do with the three-dimensional nature of the sample. As the magnetic field increased, elongated needles that do not traverse the sample increased in length to form the sample-traversing columns. Once these columns form, the dynamics slow down considerably. It is possible that the random needle structure at low fields becomes frozen over some time scale when the needles become columns and, as a result, the system has trouble reaching equilibrium even under the conditions of our experiment.

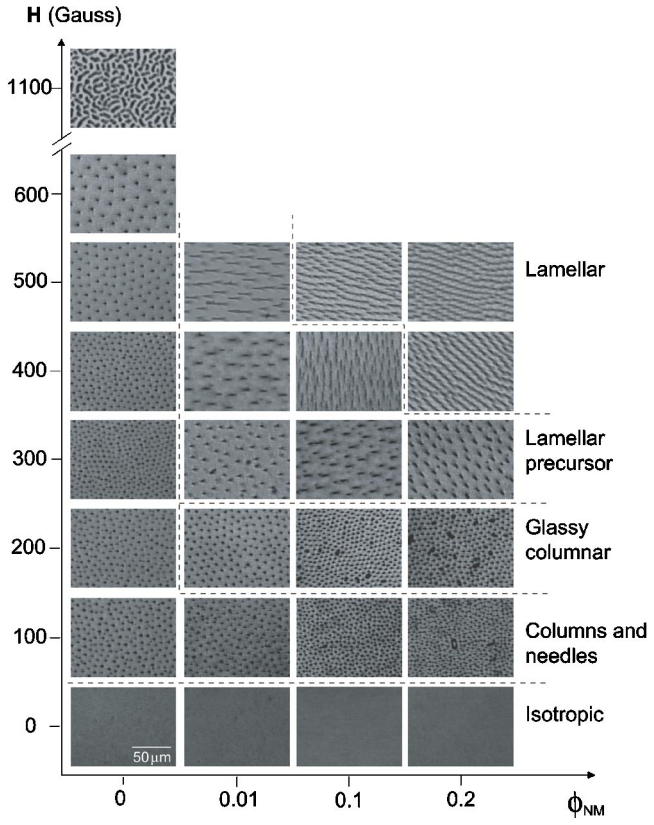

FIG. 8. Optical microscope images of how the structures formed by ferrofluid evolve when nonmagnetic latex spheres of comparable or larger diameter are added to ferrofluid suspensions. When nonmagnetic latex spheres are added to ferrofluid, the mixtures exhibit lamellar and stripe phases. These phases are predicted for ferrofluid alone system but have not been observed. The images shown here are for nonmagnetic spheres of diameter 42 nm.

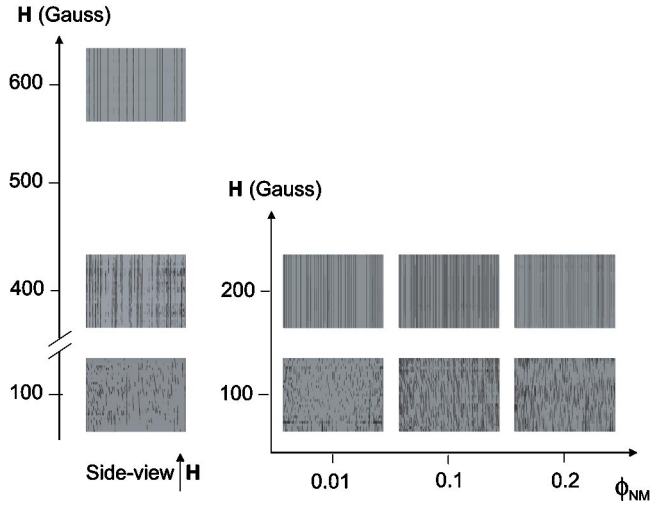

FIG. 9. Cross-sectional images through the samples (i.e., side-views) of pure ferrofluid and the mixtures exhibit the existence of needles and columns at different fields for the mixtures of ferrofluid and $d_{NM}=42$ nm beads. We also exhibit similar images of ferrofluid alone, to contrast with the effect of added nonmagnetic beads. Note, the vertical axis for ferrofluid alone is different from the mixtures. The mixtures exhibit a similar needles-to-columnar progression. The most surprising difference is that the mixtures formed almost all columns at a much lower field (200 G) than the ferrofluid (600 G).

The theory of Lacoste and Lubensky (LL) adds long-range dipolar forces to a realistic treatment of dilute hard-core colloidal fluids [17]. It makes quantitative predictions about the phase behavior of ferrofluids which are not in numerical agreement with our experiments. The dipolar interaction parameter, $\lambda=m^2/(4\pi\mu_0 d_{FF}^3 k_B T)$, where m is the magnetic moment of ferrofluid particles, μ_0 is the magnetic permeability of vacuum, k_B is Boltzmann's constant and T is the temperature, in our experiments is ~ 2.2. The LL theory, on the other hand, does not predict phase transitions for $\lambda<2.68$ (see Fig. 7). It is thus clear that our experiments cannot be interpreted completely in terms of such a two-dimensional mean-field theory. A more complete theory should include both fluctuations and inhomogeneities in the direction parallel to the fields.

B. Miscible mixtures of ferrofluid and nonmagnetic latex spheres

In this section we discuss our observations of miscible mixtures of ferrofluid and nonmagnetic latex spheres. The most significant new qualitative effects observed in the mixtures was that very small amounts of added nonmagnetic particles (i.e., $\phi_{NM}=10^{-2}$) reduce the magnetic-field strengths required for the formation of columnar and lamellar phases by $\sim 60\%-70\%$, compared to analogous phases in ferrofluid alone.

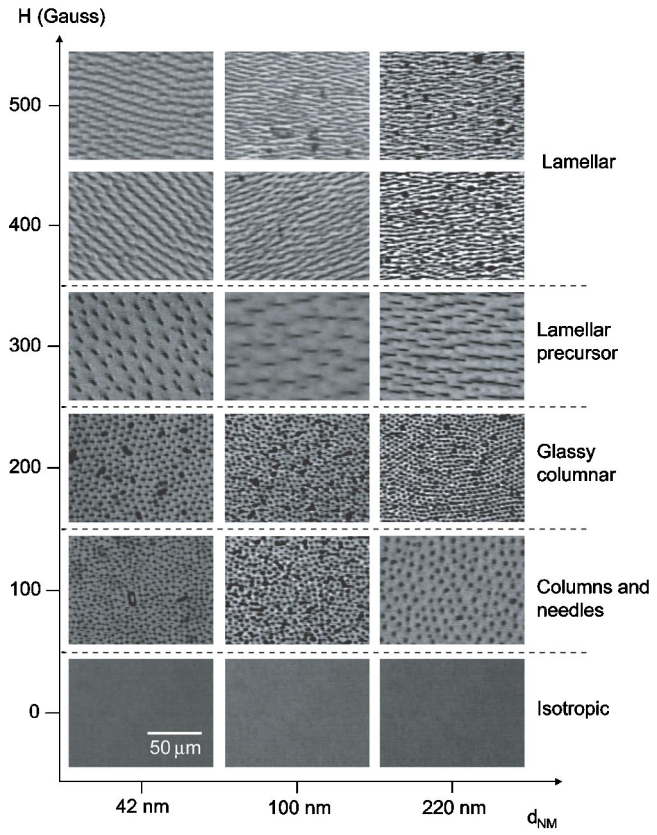

FIG. 10. Optical microscope images illustrating how the diameter of the added nonmagnetic latex spheres affects structures formed by aqueous ferrofluid suspension. Images are for nonmagnetic beads with $\phi_{FF}=20\%$ and diameter 42 nm, 100 nm, and 220 nm, respectively.

Figure 8 summarizes the primary features of our observations. These data were taken for mixtures of ferrofluid and $d_{NM}=42$-nm nonmagnetic particles. The images shown are top views taken ≈ 60 μm below the cell surface. No phase instabilities were observed in zero field at any volume fraction. Side views of the sample reveal the ferrofluid to be composed mainly of needles at 100 G (see Fig. 9); the mixtures exhibit an isotropic-to-columnar transition at ~ 200 G. The average column spacings (D) were smaller for all of the mixtures compared to pure ferrofluid at 600 G. Using the same set of image analysis tests as for ferrofluid alone, we deduced that the columnar phase was not positionally ordered. The value for Ψ_6 for the mixture at 200 G was slightly larger than that of pure FF at 600 G, but still too low to suggest long-range positional order. The columns were pinned and the phase appeared to be glassy. Ferrofluid lamellae began forming between 250 G and 300 G. At the highest fields (500 G) a pure stripe phase evolved. The phase was more robust in samples with the higher concentrations of nonmagnetic particles.

The magnetic-field-induced structures had a weak, but systematic morphological dependence on the diameter and volume fraction of the added nonmagnetic spheres. The essential features of our size-dependent observations are summarized for $\phi_{NM}=20\%$ in Fig. 10. The images reveal the same sets of phases at roughly the same field strengths. Careful analysis of the images suggests that the large particle-diameter samples enter into their new phases a bit more completely than the small particle-diameter samples at the same field strength. For example, in the glassy columnar phase of the 220 nm particles one can readily observe the prealigning of columns prior to the formation of the lamellar phase; its lamellar precursor phase is also more complete. The average column (D) and lamellar layer (L) spacings decrease with increasing ϕ_{NM} and d_{NM}. In Fig. 11 we plot D and L normalized by their value at $\phi_{NM}=1\%$ in the columnar (200 G) and lamellar (500 G) phases. D and L decrease by $\sim 25\%$–60% as ϕ_{NM} increases to 20%. Similarly, we plot D and L normalized by their value at $d_{NM}=42$ nm in Fig. 12 to illustrate the effect of nonmagnetic sphere size; D and L decrease with an increase in d_{NM}, albeit relatively weak.

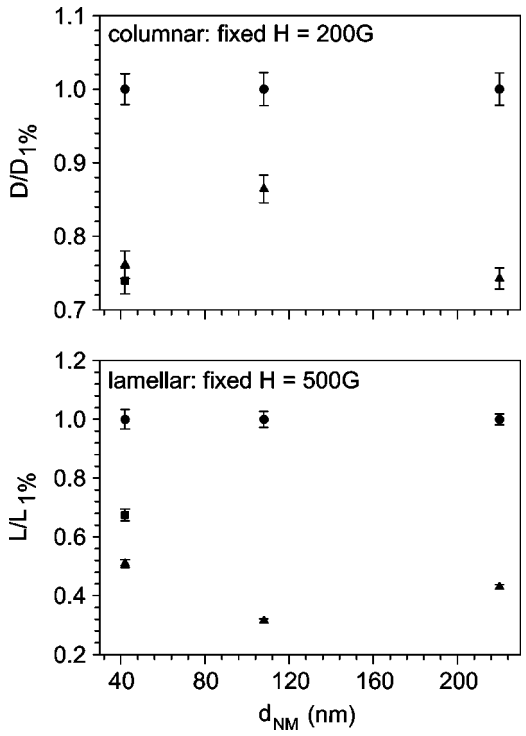

FIG. 11. D and L vs d_{NM} at different ϕ_{NM} and field strength normalized their value at $\phi_{NM}=1\%$. (●) denotes $\phi_{NM}=1\%$, (■) denotes $\phi_{NM}=10\%$, (▲) denotes $\phi_{NM}=20\%$. $D_{1\%}$ ($L_{1\%}$) is the column (lamellar) separation at $\phi_{NM}=1\%$. D and L decrease by $\sim 25\%$–60% as ϕ_{NM} increases to 20%.

The theories of Cebers [16], Halsey [5], and Lacoste and Lubensky [17] predict an isotropic-to-hexagonal/columnar-to-stripe phase sequence for pure ferrofluid. Interestingly, this phase sequence is observed in our miscible mixtures, although the columnar phase is a glassy rather than hexagonal. To our knowledge there are no theoretical predictions of phase diagrams of miscible mixtures in the literature. Our experiments show that the addition of nonmagnetic particles induces a perturbation capable of lowering the transition fields and of inducing stripe phases in this system. The origin of these qualitatively new effects is unclear.

The mean-field theory [17] writes the total free energy of the ferrofluid as a sum of four terms: an entropic energy (either in the lattice gas or the Carnahan-Starling fluid form),

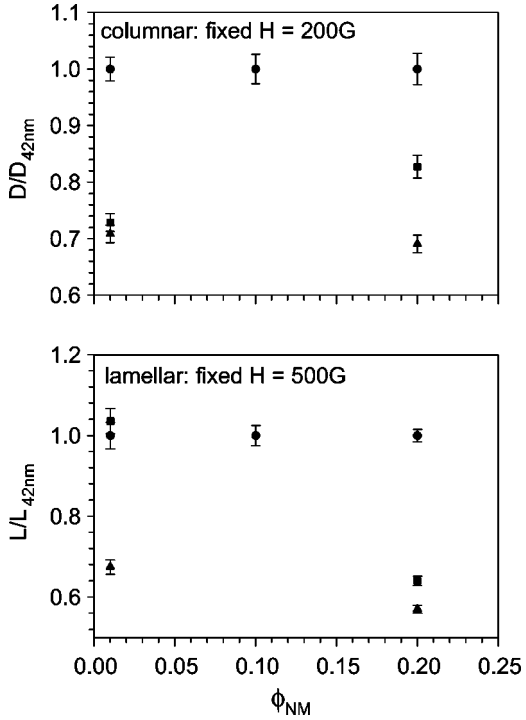

FIG. 12. D and L vs ϕ_{NM} at different d_{NM} and field strength normalized their value for $d_{NM}=42$-nm. (●) denotes $d_{NM}=42$-nm, (■) denotes $d_{NM}=100$-nm, (▲) denotes $d_{NM}=200$-nm NM beads. D_{42nm} (L_{42nm}) is the column (lamellar) separation at $d_{NM}=42$ nm. D and L decrease with an increase in d_{NM}.

a magnetic energy of magnetized particles in a magnetic field, a dipolar interaction energy between magnetic particles, and an energy cost associated with deviations of particle volume fraction from uniformity. This latter term is crucial for the prediction of phase transitions. It depends on the square of the gradient of the particle volume fraction, and its sign can be positive or negative. A related theory of mixtures will have added entropic energy and additional terms that depend on the square of the gradient of the nonmagnetic volume fraction and on the product of the gradients of the magnetic and nonmagnetic particle volume fractions. In addition, some interaction (e.g., hard sphere) must be assumed for nonmagnetic particles among themselves and for nonmagnetic particles with magnetic particles. These additional interactions can, in principle, lower the transition fields by shifting the curves in Fig. 7.

Last, we have quantitatively considered some measurable effects that might be missing from the theory, but were present in the experiments. Recall that our measurements of the sample magnetization found a small increase in the local moment of the ferrofluid particles with increasing nonmagnetic particle concentration. In principle, this effect will increase the dipolar interactions; however the change is small (of order five percent), so it is unlikely to dramatically lower the transition fields. There might also be attractive interactions between magnetic and nonmagnetic beads, because the nonmagnetic spheres have a small diamagnetic susceptibility ($\sim -7.19\times10^{-5}$). We computed the attractive interaction between a ferrofluid particle and diamagnetic particle of diameter 200 nm for our geometry (at contact), and this effect was less than 2×10^{-4} k_BT. Finally, the nonmagnetic beads can act as magnetic holes in a ferrofluid; we computed the interaction between holes of diameter 200 nm and found the largest of these energies to be ~ 0.14 k_BT. None of these effects are large enough to alter the energetics in significant ways. It is possible that there are other unaccounted attractive interactions. It is most likely, however, that phenomena embedded in the local fields or in the energy costs associated with density variations of the particle volume fractions are necessary to understand in order to elucidate the role of nonmagnetic particles.

IV. CONCLUSION

We have studied field induced phase transitions in aqueous ferrofluid and in aqueous mixtures of ferrofluid and nonmagnetic latex spheres. For ferrofluid systems, we observe the isotropic to columnar phase transition. The columns did not form a hexagonal structure, however, rather they remained in a glassy state. We do not observe any phase transition to lamellar phase, but did observe the onset of a labyrinthine structure. When nonmagnetic particles of comparable and larger diameter were added to the ferrofluid, the resulting mixtures exhibited the isotropic-columnar-lamellar phase transition at much lower fields. The column and the lamellar spacing decrease with increasing nonmagnetic particle volume fraction and with increasing nonmagnetic particle diameter. The qualitative and quantitative deviations between theory and experiment are still not well understood.

ACKNOWLEDGMENTS

We thank R.D. Kamien, A. Cebers, M. Widom, P. Heiney, and R. Perzynski for valuable discussions. We would also like to thank Jay Kikkawa for help in measuring magnetization of our samples. This work was generously supported by the NSF through the MRSEC Grant Nos. DMR 00-79909 and DMR-0203378 and partially supported by NASA, Grant No. NAG8-2172.

[1] R.E. Rosensweig, *Ferrohydrodynamics*, 1st ed. (Dover, New York, 1997).
[2] T.C. Halsey and W. Toor, J. Stat. Phys. **61**, 1257 (1990).
[3] W.R. Toor and T.C. Halsey, Phys. Rev. A **45**, 8617 (1992).
[4] J.E. Martin, J. Odinek, and T.C. Halsey, Phys. Rev. Lett. **69**, 1524 (1992).
[5] T.C. Halsey, Phys. Rev. E **48**, R673 (1993).
[6] A. Cebers, Magn. Gidrodin. **35**, 344 (1999).
[7] J.C. Bacri and D. Salin, J. Phys. (France) Lett. **43**, L771 (1982).
[8] J.C. Bacri, R. Perzynski, and D. Salin, Endeavour **12**, 76 (1988).

[9] E. Lemaire, Y. Grasselli, and G. Bossis, J. Phys. II **2**, 359 (1992).
[10] Y. Grasselli, G. Bossis, and E. Lemaire, J. Phys. II **4**, 205 (1994).
[11] E.D.R. Massart, V. Cabuil, and E. Hashmony, J. Magn. Magn. Mater. **149**, 1 (1995).
[12] F. Elias, C. Flament, J.C. Bacri, and S. Neveu, J. Phys. I **7**, 711 (1997).
[13] S. Cutilas, G. Bossis, and A. Cebers, Phys. Rev. E **57**, 804 (1998).
[14] E. Dubois, V. Cabuil, F. Boue, and R. Perzynski, J. Chem. Phys. **111**, 7147 (1999).
[15] F. Gazeau, E. Dubois, J.C. Bacri, F. Boue, A. Cebers, and R. Perzynski, Phys. Rev. E **65**, 031403 (2002).
[16] A. Cebers, Magnetohydrodynamics **37**, 195 (2001).
[17] D. Lacoste and T.C. Lubensky, Phys. Rev. E **64**, 041506 (2001).
[18] A.T. Skjeltrop, J. Appl. Phys. **57**, 3285 (1985).
[19] H. Wang, Y. Zhu, C. Boyd, W. Luo, A. Cebers, and R.E. Rosensweig, Phys. Rev. Lett. **72**, 1929 (1994).
[20] J. Liu, E.M. Lawrence, A. Wu, M.L. Ivey, G.A. Flores, K. Javier, J. Bibette, and J. Richard, Phys. Rev. Lett. **74**, 2828 (1995).
[21] C.Y. Hong, I.J. Jang, H.E. Horng, C.J. Hsu, Y.D. Yao, and H.C. Yang, J. Appl. Phys. **81**, 4275 (1997).
[22] C.Y. Hong, C.H. Lin, C.H. Chen, Y.P. Chiu, S.Y. Yang, H.E. Horng, and H.C. Yang, J. Magn. Magn. Mater. **226**, 1881 (2001).
[23] S. Banerjee, M. Fasnacht, S. Garoff, and M. Widom, Phys. Rev. E **60**, 4272 (1999).
[24] B.J. Gans, C. Blom, A.P. Philipse, and J. Mallema, Phys. Rev. E **60**, 4518 (1999).
[25] B.J. Gans, N.J. Duin, D. van den Ende, and J. Mallema, J. Chem. Phys. **113**, 2032 (2000).
[26] G.A. van Ewijk, Ph.D. thesis, Universiteit Utrecht, Utrecht, The Netherlands, 2001.
[27] J.B. Hayter, R. Pynn, S. Charles, A.T. Skjeltrop, J. Trewhella, G. Stubbs, and P. Timmings, Phys. Rev. Lett. **62**, 1667 (1989).
[28] S.W. Charles, J. Magn. Magn. Mater. **85**, 277 (1990).
[29] M. Seul and V.S. Chen, Phys. Rev. Lett. **70**, 1658 (1993).
[30] E. Blums and A.Y. Chukhov, J. Magn. Magn. Mater. **122**, 110 (1993).
[31] J.C. Crocker and D.G. Grier, J. Colloid Interface Sci. **179**, 298 (1996).
[32] C.A. Murray, *Bond-Orientational Order in Condensed Matter Systems* (Springer-Verlag, Berlin, 1992), Chap. 4, pp. 137–215.
[33] P.M. Chaikin and T.C. Lubensky, *Principles of Condensed Matter Physics* (Cambridge University Press, Cambridge, 1997).
[34] J.A. Capc and G.W. Lehman, J. Appl. Phys. **42**, 5732 (1971).
[35] P. Molho, J.L. Porteseil, Y. Souche, J. Gouzerh, and J.C.S. Levy, J. Appl. Phys. **61**, 4188 (1987).
[36] T.E. Faber, Proc. R. Soc. London, Ser. A **248**, 460 (1958).
[37] W.M. Heckl and H. Mohwald, Ber. Bunsenges. Phys. Chem. **90**, 1159 (1986).
[38] H. Gaub, V. Moy, and H.M. McConnell, J. Phys. Chem. **90**, 1721 (1986).
[39] R.M. Weis and H. McConnell, J. Phys. Chem. **89**, 4453 (1986).
[40] R.E. Rosensweig, M. Zahn, and R.J. Shumovich, J. Magn. Magn. Mater. **39**, 127 (1983).
[41] A.O. Tsebers and M.M. Maiorov, Magnetohydrodynamics (N.Y.) **16**, 21 (1980).